

MARS CLIMATE SOUNDER OBSERVATIONS OF ICE AND DUST LAYERING IN THE MARTIAN ATMOSPHERE

J. L. Benson, D. M. Kass, MCS Team, Jet Propulsion Laboratory, California Institute of Technology, Pasadena, CA, USA (jennifer.benson@jpl.nasa.gov).

Introduction:

Atmospheric dust and ice play important roles in Mars' climate. Atmospheric dust is strongly radiatively active and highly temporally and spatially variable in its abundance. Water ice clouds play an important climatological role in the martian atmosphere, water cycle, and general circulation [1, 2]. Clancy et al. [1] argued that coupled radiative/dynamical interactions involving dust aerosol and water ice clouds may have important consequences for the vertical distribution of water vapor and dust. Since water condenses on dust, cloud formation can act to remove dust, the major source of atmospheric heating, from the air. In effect, the dust layer height is efficiently limited by cloud processes [3].

Observations of the vertical distribution of aerosols at the limb from stellar occultation measurements made by Phobos 2 [4] and the Mars Express SPICAM UV spectrometer [5, 6] show detached water ice cloud layers superimposed on the background dust haze layer with dust extending high in the atmosphere during dusty times and confined near the surface (~25 km) in polar regions and during the clear season. This reveals a seasonal variability in the maximum elevation of aerosol hazes, increasing from aphelion to perihelion with a difference of more than 30 km [5, 7].

Hinson and Wilson [8] and Lee et al. [9] argue that the water ice distribution is controlled by the thermal tides. Since the saturation pressure of water vapor is a strong function of temperature, water ice will tend to condense near temperature minima such as the anti-nodes of the diurnal tide. The tidal control of the water ice results in significant changes in the location of the ice over the diurnal cycle. If the tide controls the ice in the aphelion season, the aphelion cloud belt (ACB) will shift vertically over the course of the day.

Atmospheric dust and ice have been investigated, but relatively little is known about their vertical structure. Observations of the vertical structure of ice and dust from the Mars Climate Sounder (MCS) offer a new aspect to Mars atmospheric science. The Thermal Emission Spectrometer has made limb observations [10, 11]; however these data have coarse sampling with one observation every 10°-20° of latitude around the orbit [12] compared to every ~2° in latitude for MCS [13]. The composition of aerosol hazes cannot be unambiguously distinguished from limb observations made with the SPICAM UV spectrometer [5, 6]. Consequently, MCS observations provide a more complete view of the atmos-

phere than previous data has allowed.

The MCS instrument onboard the Mars Reconnaissance Orbiter [14] makes radiance observations from pole to pole, in both the morning and afternoon, producing a profile from the surface to about 95 km. The radiances are used to retrieve vertical profiles of pressure, temperature, dust (22 μm), and water ice (12 μm). These aspects provide the necessary data to expand our knowledge of the vertical structure of ice and dust and their interaction on Mars.

Data and Methods:

We categorize and sort the ice and dust vertical profiles in three ways. The first way is by peak extinction and height (Category 1). We choose the ice layer with the highest maximum extinction and define the height of the ice at the location of the peak extinction. We define the height of the top of the dust layer as the location of the steepest slope of the dust profile. We further sort peak extinction and height into high, medium, and low groups, using the same groups for both ice and dust. The definitions of the categories are listed in Table 1.

Table 1: Dust and Ice Peak Extinction & Height Categories

Category	Dust (d) & Ice (i) Peak Extinction (km ⁻¹)	Dust (d) & Ice (i) Height (Pa)
High	$i, d > 1 \times 10^{-3}$	$i, d < 10$
Medium	$1 \times 10^{-3} > i, d > 1 \times 10^{-4}$	$10 < i, d < 100$
Low	$i, d < 1 \times 10^{-4}$	$i, d > 100$

The second way in which we categorize and sort the profiles is by the broadness of the ice layer, combined with the ice peak extinction (Category 2). We use the same definition of ice peak extinction defined in Table 1. We define the breadth of the ice layer as the distance between the top and bottom of the ice layer in scale heights, H . The top of the ice layer is the location of the steepest slope of the ice profile, and the bottom of the ice layer is the location of the smallest slope. We sort ice layer breadth into three groups:

1. Broad (see Fig. 1b): $H \geq 2$,
2. Medium (see Fig. 1c): $1 \leq H < 2$, and
3. Narrow (see Fig. 1a): $H < 1$.

The third way in which we categorize and sort the profiles is by the separation of the ice and dust layers, which we define as the distance between the bottom of the ice layer and the top of the dust (Cate-

gory 3). We sort the layer separation into four groups based on scale height, H :

1. Far apart: $H \geq 2$,
2. Medium: $1 \leq H < 2$,
3. Close (see Fig. 1c): $-0.5 \leq H < 1$, and
4. Mixed (see Fig. 1b, e): $H < -0.5$

We further separate the mixed group into “partially mixed” (Fig. 1b) and “fully mixed” (Fig. 1e).

Profiles where the top of the dust is within half a scale height of the top of the ice layer or is higher than the top of the ice layer are considered fully mixed and others are partially mixed.

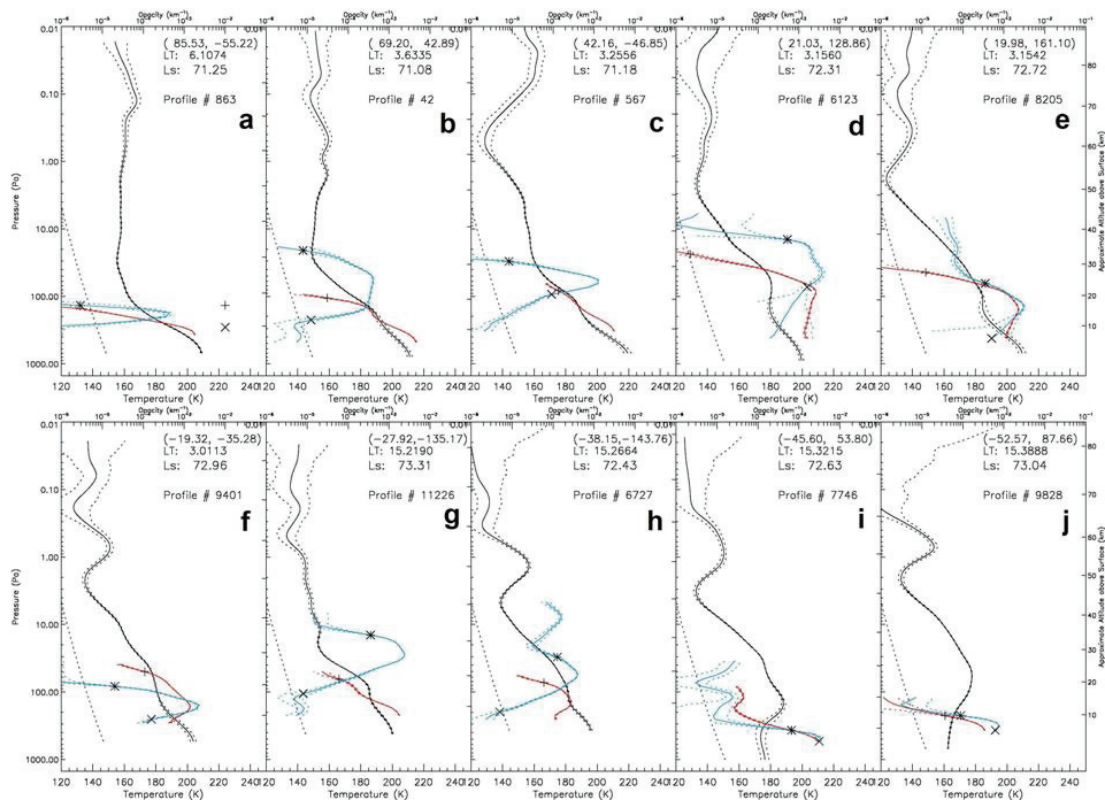
Figure 1 shows profiles of temperature (black), ice (blue) and dust (red) extinction which illustrate the category definitions given above. Symbols indicate the top of the ice layer (*), the bottom of the ice layer (X), and the top of the dust layer (+).

We then mapped the spatial distributions of the most common ice and dust configurations (# of profiles in each configuration above a threshold value and the value returns $\geq 70\%$ of the total) in the AM

Figure 2 is map for Category 1, showing the spatial distribution of water ice and dust in the Martian atmosphere at aphelion ($L_S = 71^\circ - 73^\circ$). The colors and symbols are defined in Table 2.

The majority of ice and dust configurations separate into zonal bands. These bands illustrate gradients in either extinction or height of ice or dust. Dust extinction is high in the northern hemisphere and decreases southward and is very low in the south polar hood region (poleward of $\sim -50^\circ$ S) with extinctions less than $1 \times 10^{-6} \text{ km}^{-1}$. Dust height is mostly medium ($10 < d < 100 \text{ Pa}$) except in the polar regions, where it is low. Ice extinction and height are lower in the polar regions and increase equatorward. Ice extinction is high in the tropics and mid-latitudes (yellow squares) where the ACB forms [1], although this region extends further north than is expected based on the cross-equatorial Hadley circulation [2].

We find no instances at this season where ice or dust height is high. This is consistent with previous observations of ice and dust [1, 5, 6]. The zonal pattern is likely controlled by the diurnal thermal tide



(3 am) and PM (3 pm) for each category. *Figure 1: Profiles of temperature (black), ice extinction (blue) and dust extinction (red) for regions in Figure 2. The temperature is indicated on the bottom axis while the extinction is on the top axis. The diagonal dashed line is the CO_2 condensation curve. Latitude, longitude, local time, and L_S are given at the top right of each panel.*

Results and Discussion:

[9]. Overall, the observed pattern roughly matches previous (primarily daytime) measurements.

Some configurations cluster near topographic features like volcanoes and basins. For example, ice and dust height decrease from west to east across volcanoes (e.g. Elysium Mons at 150 E, 25 N). In Valles Marineris (20-80 W, 10 S), the ice has moved lower in the atmosphere and is mixed with the dust. In Hellas (50-100 E, 20-60 S) and Argyre (30-60 W, 35-55 S) basins, aerosol extinctions decrease from

north to south.

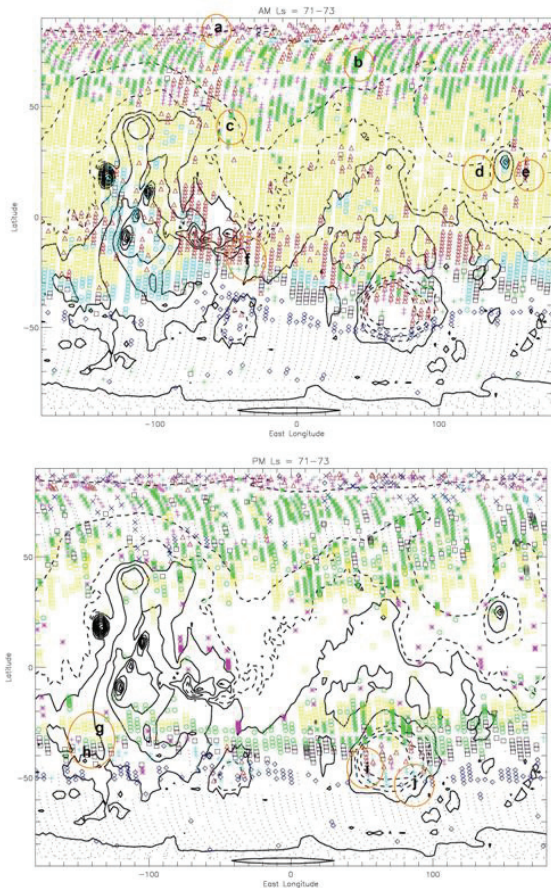


Figure 2: Map of ice and dust distributions at $L_S=71^\circ-73^\circ$ in the AM (top) and PM (bottom). The colors and symbols are defined in Table 2. Topographical contours are shown in black with dashed lines indicating negative relief. Circled letters correspond to panels in Figure 1. Black dots indicate regions of either no ice or no dust.

Figure 1 displays profiles of temperature, ice extinction and dust extinction in ten regions (circled letters) in Fig. 2. Figures 1 a-c are profiles within three adjacent zonal bands in Fig. 2 (AM) from north to south. Fig. 1a is in the north polar region where little water vapor is available [15] to condense and form clouds; hence there is a low (200 Pa), narrow ice layer with low extinction. Moving further south where more water vapor is available [12], Figs. 1 b and c exhibit higher ice layers (50 Pa) and a trend of increasing peak extinction moving southward. These ice layers have maximum extinction where there is a temperature minimum, indicative of a feedback between temperature and water ice.

Figures 1 d-f are profiles in regions where the ice and dust configurations cluster near topographic features in Fig. 2 (AM). Figure 1d is west of Elysium Mons. Ice forms higher (30 Pa) and has a more extended layer in this region than seen in Fig. 1c. The dust also extends to a higher level. Figure 1e is just east of Elysium Mons, and the ice has moved

lower in the atmosphere (100 Pa) than in Fig. 1d and is mixed with the dust. This west to east gradient in ice

Table 2: Category 1

Color and Symbol	Ice Height	Ice Extinction	Dust Top Height	Dust Extinction
Pink +	Low	Med.	Low	High
Green *	Med.	Med.	Low and Med.	High
Blue X (PM only)	Low	Low	Low	High
Yellow □	Med.	High	Low and Med.	High
Pink * (PM only)	Med.	High	Med.	Low
Green O (PM only)	Med.	High	Low and Med.	Med.
Red △	Low	High	Low and Med.	High
Cyan O (AM only)	Med.	High	Med.	Med.
Green + (AM only)	Low	Med.	Med.	Med.
Cyan + (PM only)	Low	Med.	Low	Med.
Black □	Med.	Med.	Low and Med.	Med.
Blue ◇	Low	Med.	Low	Low

height across Elysium is also shown in Fig. 2. As a high volcano, Elysium may significantly modify the local atmosphere, leading to different conditions with vertical transport playing a role [16]. Figure 1f is within Valles Marineris (red triangle), where the thickest ice layer is low in the atmosphere (200 Pa) and is mixed with the dust.

Figures 1 g-j are profiles for regions (circled letters) in Fig. 2 (PM). Figures 1 g and h show profiles from two adjacent zonal bands in Figure 2 which have decreasing dust and ice extinction moving poleward. The dust and ice profiles in Fig. 1g are very similar to those in Fig. 1c even though they are in opposite hemispheres and times of day. Figures 1 i and j show profiles in Hellas where aerosol opacity decreases from north to south deep within the basin.

Figure 3 is map for Category 2, showing the spatial distribution of ice layer breadth and ice extinction. The colors and symbols are defined in Table 3. The zonal bands due to the ice extinction are evident (as seen in fig. 2). In the tropics and mid-latitudes the ice extinction is high and there are broad, medium, and narrow layers of ice, although there are many broad layers and few narrow layers. In the north polar region, there are medium and narrow ice

layers with medium extinction and also some medium layers with high

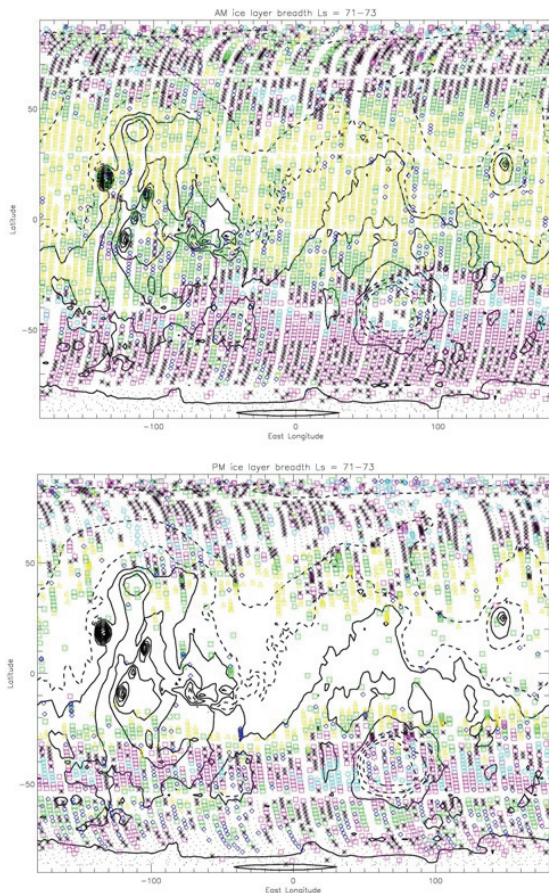


Figure 3: Same as Fig. 2 except this is a map of the spatial distribution of ice layer breadth and ice extinction. The colors and symbols are defined in Table 3.

extinction. The south polar region is dominated by narrow and medium ice layers with medium opacity.

In the AM (top) panels of figs. 2 and 3, there is a wave number 1 pattern in the distribution in the north. The pattern is mostly delineated by the green * in fig. 2 and the black * in fig. 3, both of which represent a medium ice extinction. The northern edge of the wave pattern lies at about 50° N with the peak extending to 40° N at -30° E longitude. In the south of fig. 3 (AM) there is a wave number 2 pattern in the distribution which is delineated by the black *. The edge of the wave pattern lies at about 35° S with one peak extending to 20° S at -35° E longitude and the other to 20° S at 100° E longitude.

We find that the ice and dust are nearly always mixed to some degree in the AM. From about 0° to 80° N, the ice and dust are mostly partially mixed (see fig. 1b). From 80° to 90° N and 0° to 40° S, the ice and dust are mostly fully mixed (see figs. 1a, f). There are zonal bands where ice and dust separation is mostly close between 40°-50° N and 40°-55° S (see fig. 1c). In the PM, ice and dust separation is more evenly distributed between close, partially

mixed, and fully mixed, although there are more cases of a close separation. The ice and dust separation is mostly close between 30°-80° N and 20°-50° S (see fig. 1g). The ice and dust are mostly fully mixed from 80° to 90° N, like in the AM. At both times of day, the top of the ice layer usually forms above the top of the dust, although there are some exceptions as seen in Fig. 1f.

Table 3: Category 2		
Color and Symbol	Ice Layer Breadth	Ice Extinction
Black *	Medium	Medium
Cyan O	Narrow	Low
Yellow Δ	Broad	High
Green □	Medium	High
Blue ◇	Narrow	High
Pink □	Narrow	Medium

We are performing a similar analysis for three additional seasons ($L_S=0^\circ$, 160° and 210°) to examine seasonal evolution of aerosols.

Conclusions:

We have mapped ice and dust distributions at aphelion. There is an obvious distinction between the ACB and the polar hoods at this season. The ACB itself is a complex structure. The north and south edges of the ACB are defined by bands with gradients in ice extinction. The edges of the ACB are not longitudinally uniform, but instead show latitudinal variability. The northern edge follows a wave number 1 pattern and the southern edge is defined with a wave number 2 pattern. The peak extinction in ice opacity best delineates the edges of the ACB. Within the ACB are topographic features which modify the ice and dust vertical structure.

Acknowledgements: Work at the Jet Propulsion Laboratory, California Institute of Technology, was performed under a contract with the National Aeronautics and Space Administration.

References: [1] Clancy, R.T. et al. (1996) *Icarus*, 122, 36-62. [2] Richardson, M. I. et al. (2002) *JGR*, 107, 5064. [3] Rodin, A. V. et al. (1999) 5th Internat. Conf. Mars, No. 6235. [4] Chassefière, E., J. et al. (1992) *Icarus*, 97, 46-69. [5] Montmessin, F., P. et al. (2006) *JGR*, 111, E09S09. [6] Rannou, P., S. et al. (2006) *JGR*, 111, E09S10. [7] Jaquin, F., P. et al. (1986) *Icarus*, 68, 442-461. [8] Hinson, D. P., and R. J. Wilson (2004) *JGR*, 109, E01002. [9] Lee, C., W. et al. (2009) *JGR*, 114, E03005. [10] McConnochie, T. H. and M. D. Smith (2007) 7th Internat. Conf. Mars, No. 1353, p. 3345. [11] McConnochie, T. H. and M. D. Smith (2008) 3rd Internat. Wkshp. Mars Atmos., No. 1447, p. 9114. [12] Smith, M. D. (2004) *Icarus*, 167, 148-165. [13] McCleese, D. J. et al. (2007) *JGR*, 112, E05S06. [14] Zurek, R. W. and S. E. Smrekar (2007) *JGR*, 112, E05S01. [15] Fedorova, A., O. et al. (2006) *JGR*, 111, E09S08. [16] Michaels, T. I et al. (2006) *GRL*, 33, L16201.